Int. J. Electrochem. Sci., 14 **(2019)** 4206 – 4215, doi: 10.20964/2019.05.28

International Journal of ELECTROCHEMICAL SCIENCE
www.electrochemsci.org

Self-Assembled Monolayers of Alkanethiol as Inhibitors against Copper Corrosion in Synthetic Acid Rain

Ivana Martinović[*]*, Gloria Zlatić, Zora Pilić, Lucija Šušić, Olga Kowalska, Danijel Petrović, Franjo Falak, Josip Mišković*

Department of Chemistry, Faculty of Science and Education, University of Mostar, Mostar, Bosnia and Herzegovina
[*]E-mail: ivana.martinovic@fpmoz.sum.ba

Received: 9 January 2019 / *Accepted:* 4 March 2019 / *Published:* 10 April 2019

The adsorption and corrosion inhibition of alkanethiols self-assembled monolayer on the copper surface in simulated acid rain were investigated by electrochemical techniques. Self-assembled monolayer (SAM) was formed by 1-octanethiol (OT), 1-dodecanethiol (DT) and 1-octadecanethiol (ODT) molecules on copper surface. The experimental results showed that inhibiton efficiency increases simultaneously with increase of concentration and chain length of thiols. At the concentration of 0.5 mmol L^{-1}, 1-octadecanethiol (ODT) acts as effective corrosion inhibitor with inhibition efficiency of ~ 90%. The adsorption of alkanethiol self-assembled monolayer on the copper surface was investigated by polarization measurements. The adsorption of SAMs on the copper surface followed Langmuir isotherm and the standard Gibbs energy indicated that the adsorption mechanism of OT, DT and ODT on copper is the hybrid type of physical and chemical adsorption. Values of Gibbs energy ranging from ─24 kJ mol^{-1} for OT to ─32 kJ mol^{-1} for ODT indicate that the chemisorption part in the adsorption mechanism prevails with the increase of alkanethiols chain length.

Keywords: self-assembled monolayer; copper; acid rain; electrochemical techniques

1. INTRODUCTION

Copper and its alloys have been widely used for different applications in various environments because of their excellent chemical properties. Wide application of copper has been based on its corrosion stability, which depends on the properties and stability of the surface oxide layer. The main factors, which affect the corrosion of copper, are properties and the pH of the aqueous electrolytes, as well as thickness and structure of the surface layer. It was found that the corrosion of copper is lowest in alkaline and highest in acidic solution. Stable surface oxides on copper cannot be formed at pH values below 5 [1, 2].

Self-assembled monolayers (SAMs) have been widely investigated over the past two decades [3-12]. SAMs are formed by fast spontaneous adsorption of alkanethiols onto metal surface. The SAMs on the metal surface are densely packed molecular hydrophobic barrier films that prevent diffusion of aggressive ions toward metal surface [3-5]. They are well acknowledged for great reproducibility to form highly ordered films and are easily prepared. Wetting properties of alkanthiols on copper were investigated by measuring the contact angle [6, 11]. High value of contact angle indicated that the self-assembled monolayer on copper was closely packed and had hydrophobic properties. It was also found [11] that the hydrophobicity of SAMs increases with an increase of alkanethiols chain length due to formation of more homogeneous structure which results in thicker monolayer.

Acid rain, with its low *pH* value and presence of sulphate, nitrate and other aggressive ions is one of the major factors damaging metals exposed to this acid precipitation (underground pipes, cables, bridges, vehicles). Žerjav and Milošev [13] investigated inhibition of cooper corrosion in simulated acid rain (pH = 5) by self assembled monolayer of carboxylic acids. According to their findings self assembled monolayer achieved high inhibition efficiency on copper and the inhibition efficiency increased with increasing carbon chain length of the carboxylic acids. The investigation of the atmospheric corrosion of copper protected by self-assembled monolayers of thiols with different chain lengths showed that self-assembled alkanethiols act as efficient corrosion inhibitors for copper when exposed to humidified air with addition of formic acid [14].

In the present paper, we have attempted to form SAMs of 1-octanethiol (OT), 1-dodecanethiol (DT) and 1-octadecanethiol (ODT) on copper surface and investigate their corrosion protection efficiency in simulated acid rain, pH 4.5. The electrochemical study was performed using potentiodynamic polarization (PP), cyclic voltammetry (CV) and electrochemical impedance spectroscopy (EIS).

2. EXPERIMENTAL PROCEDURE

2.1. Materials

Copper (99.97 %; Ag 11,0 ppm, Bi 0,2 ppm, Pb 0,7 ppm, Sb 0,7 ppm, As 0,6 ppm, Fe 1,9 ppm, Ni 1,4 ppm, Sn 0,4 ppm, Zn 1,6 ppm, S 2,5 ppm, Se 0,1 ppm, Te 0,2 ppm, O_2 190 ppm) and copper electrodes modified with SAMs were used as working electrode with the surface area of 0.502 cm^2. The Cu surface was abrades with emery paper to an 1200 metallographic finish, degreased in ethanol in ultrasonic bath and rinsed with ultra pure water.

The electrolyte was a simulated acid rain solution prepared with salts [15] listed in Table 1. pH was adjusted to 4.5 with 0.5 mol L^{-1} H_2SO_4. All chemicals were analytical grade and purchased from Sigma Aldrich.

Table 1. Chemical composition of the simulated acid rain solution (g L^{-1}).

NH_4NO_3	$MgSO_4 \cdot 7H_2O$	Na_2SO_4	$KHCO_3$	$CaCl_2 \cdot 2H_2O$
0.13	0.31	0.25	0.13	0.31

2.2. Preparation of monolayers on copper

Modified Cu electrodes (Cu/OT, Cu/DT and Cu/ODT) were prepared as follows: mechanically abraded and degreased Cu electrodes were etched in a 10% HNO_3 solution for 30 s, rinsed with ultra pure water and absolute ethanol and immersed into ethanolic solution of alkanethiols for a 24 h. 1-octanethiol $C_8H_{17}SH$ (OT), 1-dodecanethiol (DT), $C_{12}H_{25}SH$ and 1-octadecanethiol (ODT), $C_{18}H_{37}SH$ were used.

Used concentrations of alkanethiols were: 0.05 mmol L^{-1}, 0.10 mmol L^{-1} and 0.50 mmol L^{-1}. After the SAMs layer was formed, the electrodes was rinsed again with absolute ethanol in order to get rid of the physically adsorbed molecules and dried.

2.3. Electrochemical measurements

The electrochemical measurements were carried out in a standard three electrode cell. A platinum electrode served as the counter electrode and an Ag/AgCl, KCl 3.0 mol L^{-1} was used as the reference electrode. All the potential values refer to the Ag/AgCl electrode.

Electrochemical techniques, potentiodynamic polarization (PP), cyclic voltammetry (CV) and electrochemical impedance spectroscopy (EIS) were performed using a potentiostat Autolab PGSTAT320N controlled by Nova 1.5 software.

Cyclic voltammetry (CV) experiments were performed with the Cu and modified Cu electrodes, potential ranging from –1.5 to 0.2 V with a scan rate of 40 mV s^{-1}.

Adsorption studies were carried out with Cu and modified Cu electrodes with alkanethiol concentrations of 0.05 mmol L^{-1}, 0.10 mmol L^{-1} and 0.50 mmol L^{-1}, respectively. Adsorption of OT, DT and ODT was investigated using potentiodynamic polarization measurements. PP measurements were carried out in the wide potential range from –250 mV to 250 mV near corrosion potential with the scan rate of 1.0 mV s^{-1}.

Electrochemical impedance spectroscopy was performed at open circuit potential (E_{OCP} = – 0.016 V) in the frequency range 10 kHz – 5 mHz with a 10 mV rms amplitude. Prior to EIS measurements the electrodes were immersed in the solution for 30 minutes at the open circuit potential for stabilization. All experiments were performed at least thrice for reproducibility.

3. RESULTS AND DISCUSSION

3.1. Potentiodynamic polarization

Figure 1 illustrates the potentiodynamic polarization curves of the Cu, Cu/OT, Cu/DT and Cu/ODT electrodes in simulated acid rain solution, pH 4.5.

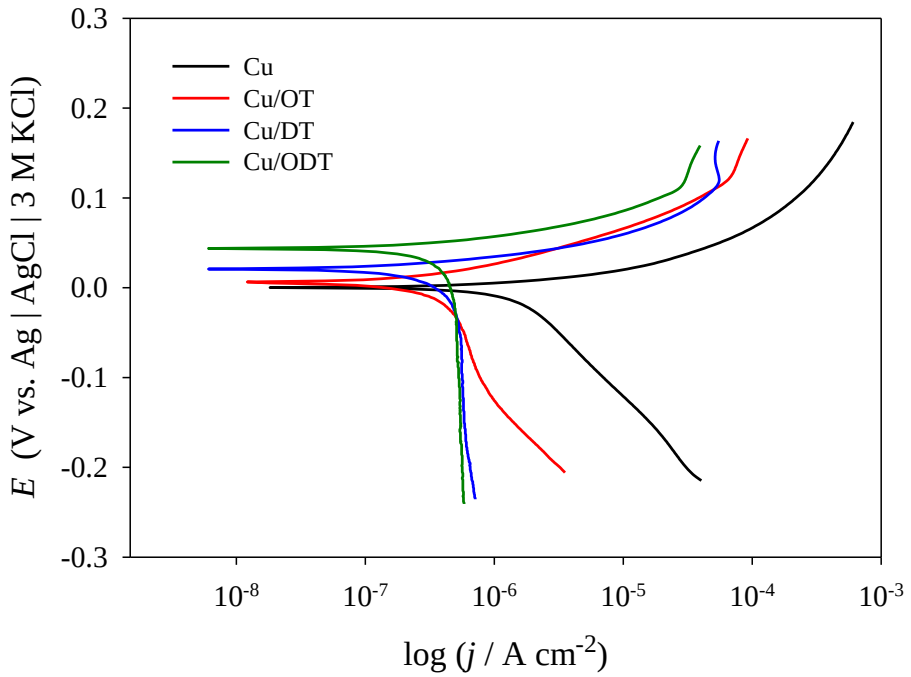

Figure 1. Potentiodynamic polarization curves of Cu, Cu/OT, Cu/DT and Cu/ODT electrodes in simulated acid rain (shown in figure); ν = 1.0 mV s^{-1}; c(OT, DT and ODT) = 0.50 mmol/L.

Figure 1 shows that the corrosion potential shifts towards more positive potentials with increase in alkanethiols chain length. The presence of SAMs cause a remarkable decrease in the corrosion rate, i.e. shifts both the anodic and cathodic curves to lower current densities compared with those of the bare Cu electrode. This suppression of the corrosion process is the results of adsorbed SAM that acts as a barrier to the ion diffusion toward copper surface.

The polarization parameters deduced from these curves by Tafel extrapolation method are presented in Table 2. The surface coverage and inhibition efficiency of SAMs were calculated using following equations:

$$\theta = \frac{j_{corr} - j_{corr(SAM)}}{j_{corr}} \quad (1)$$

$$\eta = \theta \cdot 100 \quad (2)$$

where j_{corr} and j_{corr}(SAM) represent corrosion current densities of bare copper electrode and electrode modified with SAM, respectively. Calculated values are presented in Table 2.

Table 2. Corrosion potential, corrosion density, surface coverage and inhibition efficiency of bare copper electrode and electrode modified with SAM in simulated acid acid.

electrode	E_{corr} / V	j_{corr} /A cm^{-2}	θ	η / %
Cu	0.022	$1.34 \cdot 10^{-6}$	-	-
Cu/OT	0.028	$3.17 \cdot 10^{-7}$	0.763	76.3
Cu/DT	0.036	$2.27 \cdot 10^{-7}$	0.831	83.1
Cu/ODT	0.049	$1.90 \cdot 10^{-7}$	0.858	85.8

The corrosion inhibition mechanism and the interaction between investigated alkanethiols and copper surface can be studied by the adsorption isotherms. The degrees of surface coverage (θ) for various concentrations of selected alkanethiols were determined by potentiodynamic polarization (PP curves is not presented) and calculated according to the equation 2.

The obtained experimental data were tested graphically to fit different isotherms, to explain the relationship between the surface coverage θ and the concentration of the adsorbed molecules. It was found that the obtained results can be described with the Langmuir isotherm that is given by the following equation:

$$\frac{c}{\theta} = \frac{1}{K_{ads}} + c \quad (3)$$

where c is the inhibitor concentration, θ is the degree of surface coverage and K_{ads} is the adsorption constant [16]. Linear dependence of c/θ versus c, with the slope close to 1, shown in Fig. 2, justifies the application of the Langmuir adsorption isotherm.

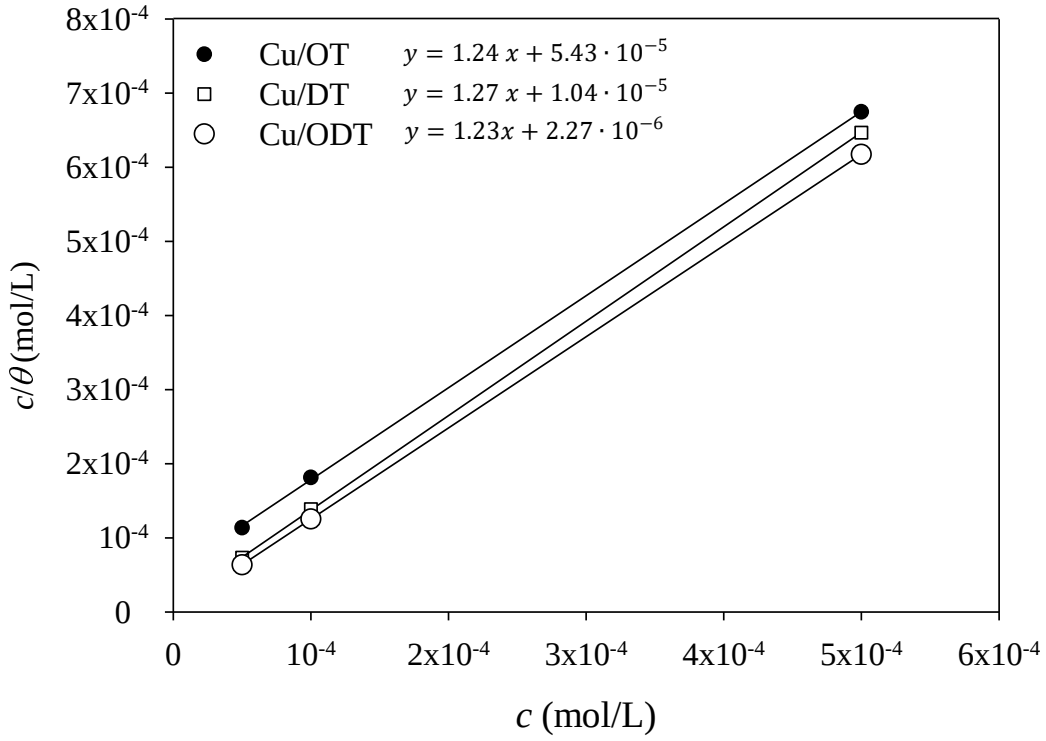

Figure 2. The Langmuir isotherm adsorption plots for SAMs formed at the copper surface in acid rain solution.

The relationship between the adsorption constant and the Gibbs energy of adsorption, ΔG_{ads} is given by [16]:

$$\Delta G_{ads} = -RT \ln K_{\text{ads}} \quad (4)$$

where R is the general gas constant (8.314 J mol^{-1} K^{-1}) and T is the absolute temperature (298.15 K).

The adsorption constant and the Gibbs energy were determined as follows: for OT: K_{ads} = $1.84 \cdot 10^4$ and ΔG_{ads} = –24.33 kJ mol^{-1}; for DT: K_{ads} = $9.62 \cdot 10^4$ and ΔG_{ads} = –28.43 kJ mol^{-1} and for

ODT: K_{ads} = 4.41·10^5 and ΔG_{ads} = –32.20 kJ mol^{-1}. The high values of K_{ads} indicate the high adsorption ability of selected alkanethiols on copper surface.

The negative values of o ΔG_{ads} ensure the spontaneity of the adsorption process and stability of the adsorbed layer on the metal surface. According to the values of standard free energy, it is possible to determine the type of adsorption. The values of ΔG_{ads} around –20 kJ mol^{-1} or lower belongs to a physisorption, while values more negative than 40 kJ mol^{-1} are associated to chemisorptions by charge sharing or transfer from the inhibitor molecules to the metal surface to form a coordinate type of bond [16-19]. Calculated values of ΔG_{ads} indicate that the adsorption mechanism of OT, DT and ODT on copper is the hybrid type of physical and chemical adsorption. Chemisorption part in the adsorption mechanism prevails with the increase of alkanethiols chain length.

3.2. C yclic voltammetry

Cyclic voltammograms for the Cu, Cu/OT, Cu/DT and Cu/ODT electrodes in simulated acid rain solution, pH 4.5, are shown in Figure 3.

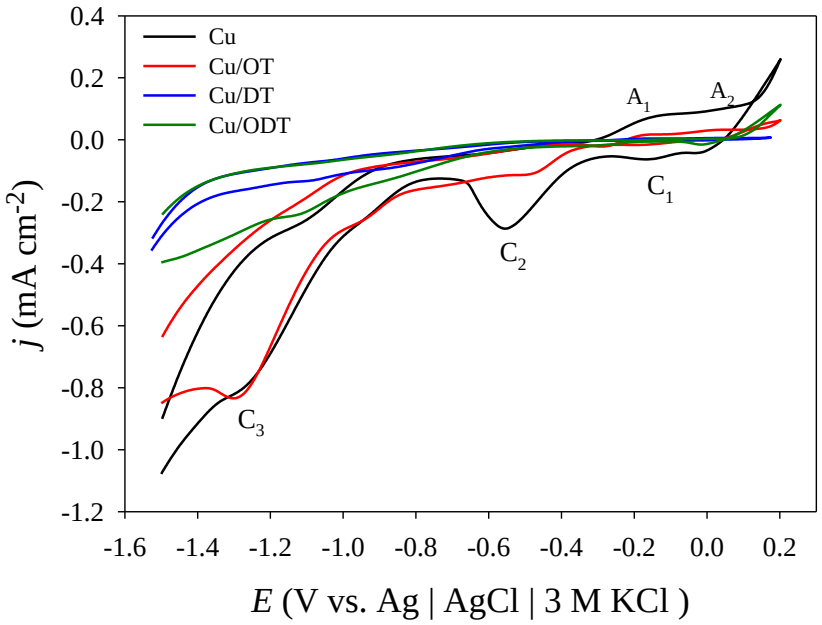

Figure 3. Cyclic voltammograms of Cu, Cu/OT, Cu/DT and Cu/ODT electrodes in simulated acid rain (shown in figure); ν = 40 mV s^{-1}; c(OT, DT and ODT) = 0.50 mmol/L.

The cyclic voltamograms were recorded within the narrow potential range (–1.50 to 0.20 V) where the initial film formation and its reduction occur. During the anodic scan the current profile on Cu electrode shows two anodic peaks. The first oxidation peak, A_1, at around –0.20 V, corresponds to the electroformation of a hydrous Cu_2O layer [1]. The second anodic peak A_2, at around 0.10 V can be ascribed to the formation of a CuO oxide [1, 20]. The reduction scan shows three current peaks. Reduction peaks C_1 and C_2 are related to the reduction of Cu(II) to Cu(I) and Cu(I) to Cu(0), respectively [20]. A third cathodic peak (C_3) close to the beginning of the hydrogen evolution region

has been associated to the reduction of soluble Cu(I) species [21-23]. For the OT, DT and ODT monolayer covered electrode, the oxidation and reduction processes are inhibited remarkably. The inhibition efficiency, η_{SAM} is calculated using the equation:

$$\eta = \frac{j_{Cu} - j_{Cu/SAM}}{j_{Cu}} \quad (5)$$

Where j_{Cu} and $j_{Cu/SAM}$ are the anodic current densities measured at 0.05 V on the Cu, Cu/OT, Cu/DT and Cu/ODT, respectively. The calculated values of inhibition efficiency of OT, DT and ODT SAMs were 69.02, 88.81 and 90.97%, respectively. These results indicate that the alkanethiol monolayer acts as an effective barrier against acid rain corrosion due its closely packed structure and high hydrophobicity. It has been found [11, 24, 25] that thiol SAMs on Cu surfaces slow down surface oxidation and the protection can be improved by using alkanethiols with longer chain length.

3.3. Electrochemical impedance spectroscopy

The electrochemical properties of the surface film formed on the bare copper electrode and on modified electrodes in simulated acid rain at the open circuit potential were investigated using EIS. Impedance spectra are presented in Fig. 4 as Nyquist plots. The standard procedures for the selection of EEC best-fit were followed: the χ^2 error was suitably low ($\chi^2 \leq 10^4$) and the errors associated with each element were up to 5 %. The ohmic resistance (R_Ω) was 50 Ω cm^2.

The Nyquist plot of the bare copper electrode shows semicircle in the medium frequency region, which is associated with the thickness and dielectric properties of surface film and the Warburg impedance in the low frequency region. The Warburg resistance in the low frequency region is ascribed to the transfer of ions to the copper surface.

The data obtained by fitting the EIS spectra of bare Cu and modified Cu electrodes to electrical equivalent circuits given in insert of Fig. 4., are presented in Table 3.

EEC consists of ohmic resistance, R_Ω in a serial connection with two time constants. The first time constant *(R* CPE_1), in the medium frequency region, is the result of a charge transfer process at the copper/acid rain interface. For fitting the spectra capacitive element is represented by constant phase element (*CPE*) due surface defects and roughness [26, 27]. Its impedance is described by the expression: $Z_{CPE}(\omega) = \left[Q(j\omega)^n\right]^{-1}$, where *Q* is a constant, ω is the angular frequency and *n* is the CPE power. Values of *n* varies from –1 and 1 [28]; a value of –1 is characteristic for an inductance, a value of 1 corresponds to a capacitor, a value of 0 corresponds to a resistor, and a value of 0.5 can be assigned to diffusion phenomena and represents a Warburg impedance [29].

The second time constant, in the low frequency region is represented by Warburg impedance.

For the SAM covered copper electrode, the diameter of the capacitive loop enlarges gradually with increasing alkanethioles chain length indicating formation of more densely packed protective film. The larger the diameter of the capacitive loop, the more difficult the electrons travel through the SAMs, and consequently the better the corrosion inhibition of SAMs [7].

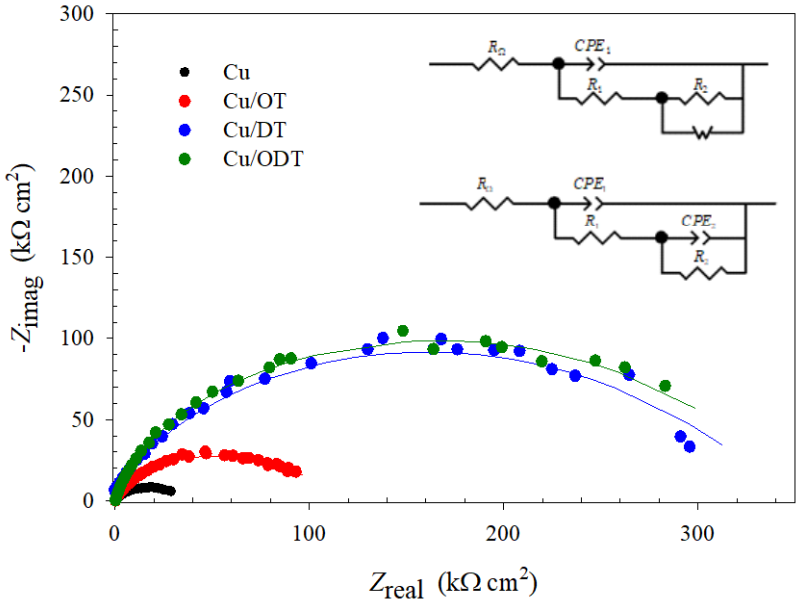

Figure 4. Nyquist plots of Cu, Cu/OT, Cu/DT and Cu/ODT electrodes in simulated acid rain (shown in figure); *c*(OT, DT and ODT) = 0.50 mmol/L.

Table 3. The numerical values of impedance parameters for Cu, Cu/OT, Cu/DT and Cu/ODT electrodes in simulated acid rain at E_{OCP}.

electrode	$Q_1 \times 10^6$ / $\Omega^{-1}s^n$ cm^{-2}	n_1	R_1 / kΩ cm^2	R_2 / kΩ cm^2	$W \times 10^{-6}$/ $\Omega^{-1}s^n$ cm^{-2}	$Q_2 \times 10^6$ / $\Omega^{-1}s^n$ cm^{-2}	n	η /%
Cu	18.139	0.830	2.177	31.458	59.758			
Cu/OT	1.068	0.788	9.899	117.845	-	4.052	0.325	73.67
Cu/DT	0.525	0.845	47.808	298.123	1.377			90.28
Cu/ODT	0.469	0.861	132.453	227.049	2.168			90.64

Compared to bare copper electrode Q_1 values tend to decrease (from 18.12 to 0.47 $\Omega^{-1}s^n$ cm^{-2}) and the R_1 and R_2 increase (from 33.63 to 359.50 kΩ cm^2) with the increase in chain length of alkanethiol (Table 3). The presence of the SAMs on the Cu electrode decreased Warburg value which means that the diffusion of species is reduced by densely packed self assembled monolayer.

The inhibition efficiency, η_{SAM} is calculated using the equation:

$$\eta = \frac{R_{Cu/SAM} - R_{Cu}}{R_{Cu/SAM}} \quad (6)$$

where $R_{Cu/SAM}$ and R_{Cu} are the resistance values of surface film. The inhibition efficiency of the OT, DT and ODT SAMs are shown in Table 3. The EIS experimental results suggest that the Cu/ODT

electrode presents the highest inhibition property, which is in good agreement with the PP and CV measurements. It has been reported [30, 31] that the thiols SAMs with chain lengths of 16 carbons or more ($n \geq 16$) exhibit more crystalline nature and greater coating resistances than SAMs with $n \leq 12$ due to long-chain thiols had greater dispersion force interactions.

The chain length of the alkanethiol determines its capacitance, and by Helmholtz model of the interface, the film capacitance is related to its thickness by the equation:

$$C_{\mathrm{SAM}} = \frac{\varepsilon_0 \varepsilon_{\mathrm{SAM}} A}{d_{\mathrm{SAM}}} \quad (7)$$

where ε_0 is the permittivity constant with the value $8.854 \cdot 10^{-12}$ F m^{-1}, $\varepsilon_{\mathrm{SAM}}$ the relative permittivity of SAM with the value of 2.1 [32], A the geometrical surface area of the electrode and d_{SAM} is the thickness of the monolayer.

The monolayer thickness is calculated using the C-C and C-S bond lengths ($l_{\mathrm{C\text{-}C}} = 1.541 \cdot 10^{-10}$ m, $l_{\mathrm{C\text{-}S}} = 1.817 \cdot 10^{-10}$ m) and the value obtained is: for OT $1.260 \cdot 10^{-9}$ m; for DT $1.877 \cdot 10^{-9}$ m and for ODT $2.801 \cdot 10^{-9}$ m. With these values, the capacitance of the SAMs is as follows: for OT 1.476 μF cm^{-2}; for DT 0.991 μF cm^{-2} and for ODT 0.664 μF cm^{-2}. The calculated values are in good agreement with the values presented in Table 3.

4. CONCLUSION

Self-assembled monolayers of 1-octanethiol (OT), 1-dodecanethiol (DT) and 1-octadecanethiol (ODT) on the copper surface show very good corrosion inhibition in simulated acid rain. The adsorption kinetics of selected alkanethiols on copper surface were studied by polarization measurements in consideration of different concentrations (0.01, 0.10 and 0.5 mmol L^{-1}) and different alkyl chain length (n = 8, 12 and 18). It was found that the adsorption process follows Langmuir adsorption model, independent of chain length of thiols. Calculated values of Gibbs energy indicated that the adsorption mechanism of OT, DT and ODT on copper is the hybrid type of physical and chemical adsorption. Increasing value of Gibbs energy from ─24 kJ mol^{-1} for OT to ─32 kJ mol^{-1} for ODT indicate that the chemisorption part in the adsorption mechanism prevails with the increase in chain length of alkanethiols.

ACKNOWLEDGEMENTS
This research was financially supported by the Federal Ministry of Education and Science of Bosnia and Herzegovina.

References

1. M. Metikoš -Huković, R. Babić and I. Paić, *J. App. Electrochem*., 30 (2000) 617.
2. V. Brusić, M.A. Frisch, B.N. Eldridge, F.P. Novak, F.B. Kaufman, B.M. Rush and G.S. Frankel, *J. Electrochem. Soc*., 138 (1991) 2253.
3. P. Durainatarajan, M. Prabakaran, S. Ramesh and V. Periasamy, *Mater. Today Proc.*, 5 (2018) 16226.
4. Y. Qiang, S. Fu, S. Zhang, S. Chen and X. Zou, *Corros. Sci.*, 140 (2018) 111.

5. M. Flores, S. Donoso, M. Ortiz, G. Acosta and H. Fernandez, *Mater. Chem. Phys.*, 208 (2018) 97.
6. S. Hu, Z. Chen and X. Guo, *Materials*, 11 (2018) 1225. doi:10.3390/ma11071225
7. H. Yu, C. Li, B. Yuan, L. Li and C. Wang, *Corros. Sci.*, 120 (2017) 231.
8. F. Xu, J. Yang, R. Qiu , J. Hou, J. Zheng, J. Zhang, L. Wang, Z. Sun and C. Lin, *Prog. Org. Coat*., 97 (2016) 82.
9. M. Metikoš-Huković, R. Babić, Ž. Petrović and D. Posavec, *J. Electrochem. Soc*., 154 2 (2007) C138.
10. C. Li, L. Li and C. Wang, *Electrochim. Acta*, 115 (2014) 531.
11. Ž. Petrović, M. Metikoš-Huković and R. Babić, *Prog. Org. Coat*., 61 (2008) 1.
12. W. Liu, W. Cao, X. Deng, Y. Min and Q. Xu, *Int. J. Electrochem. Sci*., 10 (2015) 8858.
13. G. Žerjav and I.Milošev, *Corros. Sci*., 98 (2015) 180.
14. S. Hosseinpour, M. Forslund, C.M. Johnson, J. Pan and C. Leygraf, *Surf. Sci.*, 648 (2016) 170.
15. G. Seufert, V. Hoyer, H. Wollmer and U. Arndt, *Environ. Pollut*., 68 (1990) 205.
16. Ž. Petrović, M. Metikoš-Huković and R. Babić, *J. Electroanal. Chem*., 623 (2008) 54.
17. C. Li, X. Guo, S. Shen, P. Song, T. Xu, Y. Wen and H-F. Yang, *Corros. Sci*., 83 (2014) 147.
18. M.A. Hegazy, A.M. Badawi, S.S. Abd El Rehim and W.M. Kamel, *Corros. Sci*., 69 (2013) 110.
19. M. Behpour, S.M. Ghoreishi, N. Soltani, M. Salavati-Niasari, M. Hamadanian and A. Gandomi, *Corros. Sci*., 50 (2008) 2172.
20. R. Babić, M. Metikoš-Huković and M. Lončar, *Electrochim. Acta*, 44 (1999) 2413.
21. M.B. Valcarce and M. Vazquez, *Corros. Sci*., 52 (2010) 1413.
22. M.B. Valcarce, S.R. de Sanchez and M. Vazquez, *J. Mater. Sci*., 41 (2006) 1999.
23. M.B. Valcarce, S.R. de Sanchez and M. Vazquez, *Corros. Sci*., 47 (2005) 795.
24. O. Azzaroni, M. Cipollone, M.E. Vela and R.C. Salvarezza, *Langmuir*, 17 (2001) 1483.
25. C. Vericat, M.E. Vela, G. Corthey, E. Pensa, E. Cortes, M.H. Fonticelli, F. Ibanez, G.E. Benitez, P. Carro and R.C. Salvarezza, *RSC Adv*., 4 (2014) 27730.
26. R.M. Souto, I.C. Mirza Rosca and S. Gonzales, *Corrosion*, 57 (2001) 300.
27. J.R. Macdonald, Impedance spectroscopy, emphasizing solid materials and systems, Wiley, (1987) New York, USA.
28. U. Rammelt and G. Reinhard, *Electrochim. Acta*, 35 (1990) 1045.
29. M. Metikoš-Huković, Z. Pilić, R. Babić and D. Omanović, *Acta Biomater*., 2 (2006) 693.
30. G.K. Jennings, J.C. Munro, T.H. Yong and P.E. Laibinis, *Langmuir*, 14 (1998) 6130.
31. Y. Zhanga, J. Zhoub, X. Hana, X. Zhanga and J. Hu, *App. Surf. Sci*., 353 (2015) 979.
32. K.A. Peterlinz and R. Georgiadis, *Langmuir*, 12 (1996) 4731.